Optics and Laser Technology 94 (2017) 59–67

Contents lists available at ScienceDirect

Optics and Laser Technology

journal homepage: www.elsevier.com/locate/jolt

Full length article

Correlation of high power laser welding parameters with real weld geometry and microstructure

Sang Liu [a], Gaoyang Mi [a], Fei Yan [a], Chunming Wang [a,*], Ping Jiang [b]

[a] School of Materials Science and Engineering, Huazhong University of Science and Technology, Wuhan 430074, China
[b] School of Mechanical Science and Engineering, Huazhong University of Science and Technology, Wuhan 430074, China

ARTICLE INFO

Article history:
Received 2 September 2016
Received in revised form 3 January 2017
Accepted 5 March 2017

Keywords:
High power laser welding
Shape factors
Microstructural heterogeneity
Grain boundary characterization
Texture evolution

ABSTRACT

High power laser welding has exhibited tremendous advantages over traditional arc or plasma welding over last decades. However, there still exist microstructural heterogeneity in fusion zones (FZ) and heat affected zones (HAZ), as well as loosening of the grain boundary and structural defects, which would lead to the mechanical property discontinuity of whole welded components and eventually affect the service performances. In this paper, the effect of welding parameters on the weld shape, microstructure, element distribution and texture evolution was studied under high power laser ranging from 5 kW to 9 kW on 7 mm thickness plates of SUS201 with bead-on-plate configuration. The results show that single variations of welding parameters could result in great changes of weld transverse profiles and three typical shapes of welds, including the Peanut-shaped welds (PWs), Nail-shaped welds (NWs) and Wedge-shaped welds (WWs), were summarized out according to the self-established shape factors. Relationships between welding parameters with weld shapes were preliminarily established with the help of optical microscopy (OM) and correlations between typical weld shapes with the distribution & morphology of microstructures were also explored quantitatively by SEM and EBSD tests.

1. Introduction

Joining technique is one of the important manufacturing routes that can be used to refine product design and reduce production cost. However, it still faces many challenges. Traditionally, gas tungsten arc welding (GTAW) is widely adopted in industry area and now existing IIW FFS (Fitness-for-Service) procedures mainly apply to arc-welded steel structure [1,2]. As a relative newly developed method, laser beam welding (LBW), with advantages of highly concentrated heat source, high welding speed and convenience for automation, has attracted enormous interest in recent years. The practical applications into various materials, such as steels, aluminum alloys & titanium alloys and different techniques, such as autogenous welding, filler wire welding & laser-arc hybrid welding have also been studied extensively [3–7]. Unfortunately, due to the characteristics stated above, the weld seam appearance, microstructure transformation and residual stress distribution are not all the same as that presented in arc welding [8,9]. Moreover, the laser processing itself is notably affected by a series of factors including laser beam quality, welding parameters and interactions between the irradiation and the material. The results obtained disperse and thus it is still a hard work to systematically investigate the technological properties of laser welding and their effects on typical joint performances including corrosion resistance and mechanical properties, especially in the welding of medium plates (4–25 mm thickness) under high power lasers.

Weld geometry is the most intuitive reflection of the welding process and most of basic researches usually refer to this topic inevitably. The influence of fiber laser welding conditions such as welding speed and defocusing distance on the weld bead geometry of thick stainless steels has been investigated and wine-cup bead geometry are finally obtained at low welding speed [10]. And masses of papers have reported that at higher welding speed, the laser power density exerts a significant effect on the increase of weld penetration. Welds without defects such as porosity, humping or underfilling could be produced at wide process windows [11,12]. Empirical data-based statistical analyses, model-based analytic methods and finite element simulation have also been utilized to predict the weld depth and width from different aspects [13–15]. However, weld geometry varies throughout the whole thickness. Representation just with penetration and surface width to assess the effects of welding parameters seems a bit oversimplified.

Joint microstructure, on which the operating performances of welding joints rely, has always been the fundamental evaluation

* Corresponding author.
E-mail address: hustwangcm@sina.com (C. Wang).

http://dx.doi.org/10.1016/j.optlastec.2017.03.004
0030-3992/

criteria of joint property. It was reported that in the laser welding of austenitic stainless steels, solidification mode was changed when welding speed varied, which would result in micro segregation of alloying elements and microstructure variations. Commonly, the weld maintained to be original austenitic structure, but with narrow HAZ and finer grains [16–18]. Researches in the laser welding of magnesium alloys achieved equiaxed dendrites in the central and columnar dendrites on both sides. Moreover, EBSD maps of the joints showed that grains in the FZ oriented randomly, while the base metal (BM) exhibited a strong basal texture with the {0 0 2} plane normal parallel to the sample normal direction [19]. But this influence depends, for crystallographic texture of columnar grain zone will change with increasing the welding speed [20]. Laser beam welded age hardenable aluminum alloys generally consisted of fine grained dendritic microstructure in the FZ and a narrow HAZ with coarsed strengthening precipitates at the grain boundaries, which was very similar with that in electron beam welding [21,22]. Obviously, high solidification and cooling rate induced by the specific processing lead to a distinct microstructure constitution and distribution compared with previous experience. However, most of the studies are aimed at certain process condition and the effect of microstructure on dynamic load performances, like joint fatigue fracture, is still not well known yet.

In present work, the effect of welding parameters on the weld geometry and corresponding microstructure distribution, phase transformation, chemical composition and texture evolution was discussed under the impingement of high power lasers. SUS201 was chosen as the test material, for this alloy is widely used in industries of fabrication due to its equivalent performances with SUS304 and relatively cheap cost. Weld transverse shapes were given more attention, and a simple geometric model was established. Moreover, based on this, an attempt on the relationship between welding parameters-weld shapes-microstructure characterizations was preliminarily explored. This kind of correlation from the macroscopic profile, to the mesoscopic melt pool, to the microscopic structure, not only helps to promote further understandings of the effect of high power laser, but also establish a technical and theoretic basis for the following performance analysis and practical application.

2. Experimental procedures

The base material is a commercially available SUS201 of 7 mm thickness with the delivery state of hot-roll annealing. The samples were cut into a dimension of 200 × 100 × 7 mm, with the nominal composition of the steel listed in Table 1. Before welding, the oxidation film and greasy dirt on the surface of the substrate were eliminated by mechanical wire brushing and acetone wiping. IPG YLS-10,000 fiber laser with a maximum output power of 10,000 W was applied in the experiment and the main technical parameters were present in Table 2. A series of bead-on-plate autogenous welding experiments were conducted, with the tilt angle of 8°for the laser beam and 50° for the gas tube (inner diameter 6 mm), both opposite to the welding direction. As practical applications in medium or thick plates (more than 25 mm) always call for full penetration, only those joints that presented complete penetration were picked out from all of the results as targets of interest. Pure Ar was used as the shielding gas and detailed welding parameters were given in Table 3.

Table 2
IPG YLS-10,000 fiber laser specification.

Technical parameters	Typical value
Nominal output power	10 kW
Emission wavelength	1070 nm
Working fiber core diameter	200 μm
Collimation lens focal length	125 mm
Focusing lens focal length	300 mm

Table 3
Welding parameters value ranges of bead-on-plate experiments.

Welding parameters	Value ranges
Laser power	5–9 kW
Welding speed	15–45 mm/s
Defocusing distance	−8 to +8 mm
Shielding gas flow rate	Ar, 25 l/min

After welding, metallographic specimens were prepared according to standard procedures. They were polished and etched with a solution of 3 ml HF, 9 ml HNO_3 and 12 ml H_2O. The etched samples were then observed by a stereo microscope for weld profile and by a metallographic microscope for microscopic structure. Based on the real weld shape features, all of the weld shapes can be split into three parts including the upper trapezium, the middle rectangle and the bottom trapezium, just as illustrated in Fig. 1. This kind of model could not only completely describe the weld profile, but also reflect geometric characteristics of different areas. The weld transverse geometry, i.e. the width on the upper surface (W_U), the width of middle rectangle (W_M), the width on the bottom surface (W_B) and the height of upper trapezium (H_U), the height of middle rectangle (H_M), the height of bottom trapezium (H_B), was then quantitatively measured by the included software packages and analyzed in terms of certain shape parameter combinations and process parameter combinations. The ratio of width on the bottom surface to upper surface (W_B/W_U) and the ratio of the height of middle rectangle to the whole plate thickness ($H_M/H_U + H_M + H_B$) are selected as weld shape factors in the aim of effectively

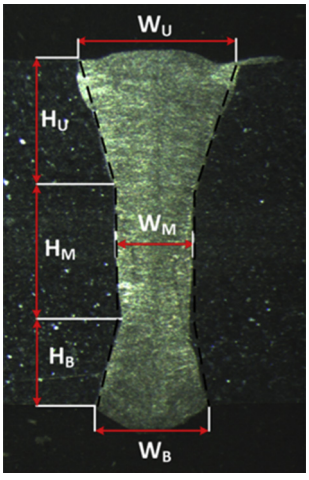

Fig. 1. Weld transverse shape model.

Table 1
Nominal chemical compositions of SUS201 (wt.%).

C	Si	Mn	Cr	Ni	N	Cu	P	S	Fe
0.08	0.53	9.06	14.57	1.02	0.147	1.52	<0.005	<0.005	Balance